ACS APPLIED POLYMER MATERIALS

pubs.acs.org/acsapm

Article

Vanillin-Based Polymers via Ring-Opening Metathesis Polymerization

Byungjin Koo*

Cite This: *ACS Appl. Polym. Mater.* 2024, 6, 1653−1661

Read Online

ACCESS | Metrics & More | Article Recommendations | Supporting Information

ABSTRACT: Biobased polymer synthesis is becoming an indispensable research area aimed at addressing environmental pollution and the depletion of petroleum resources. Vanillin, which can be sustainably obtained from lignin biomass, is a phenolic compound that is widely used as a food additive. We herein report our study of polymer synthesis using vanillin through ring-opening metathesis polymerization (ROMP). Our initial step involves the chemical transformation of vanillin into vanillin 5-norbornene-2-carboxylate (**VN**), a polymerizable monomer. This ROMP monomer has the capability to form poly(vanillin 5-norbornene-2-carboxylate) using a Grubbs catalyst. This glassy homopolymer has a molecular weight of 49,000 g/mol with a $Đ$ of 1.23. To explore its potential in copolymers, we performed triblock copolymerization to create ABA-type thermoplastic elastomers. To achieve this, we synthesized three ROMP monomers serving as soft blocks, each containing different alkyl chains. Through a sequential addition of monomers (**VN**, soft block, and **VN** in that order), we successfully synthesized six vanillin-based triblock copolymers with molecular weights of 32,000−61,200 g/mol and $Đ$ values of 1.24−1.40. These synthesized polymers exhibit excellent mechanical properties, including a Young's modulus of 28 MPa, surpassing commercial thermoplastic elastomers. Atomic force microscopy (AFM) reveals microphase separation consistent with the two distinct glass transition temperatures.

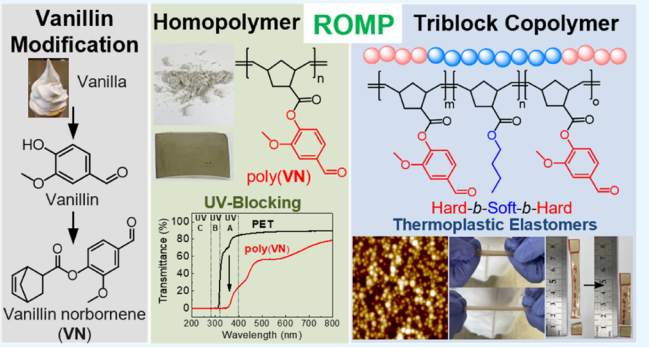

KEYWORDS: *biomass, copolymerization, ring-opening metathesis polymerization, thermoplastic elastomer, vanillin*

1. INTRODUCTION

Exploring renewable resources to produce useful polymers is critical in order to meet the ever-increasing demand for synthetic materials, prepare for potential shortages of petroleum-based raw chemicals, and reduce greenhouse gas emissions for cleaner environments.[1−3] Many biobased resources, such as terpenes,[4] vegetable oils,[5] and sugars,[6] have been extensively researched for the production of synthetic polymers.[7−13] Some of these polymers have been commercialized, as evidenced by notable examples such as poly(lactic acid)s[14−18] and polyhydroxyalkanoates.[19,20] However, their mechanical properties are often not robust due to the absence of aromatic moieties. Thus, the search for aromatic building blocks available in nature is essential to diversifying the range of available materials. One such building block can be obtained from polyphenols found in lignin[21] and tannins,[22] which are structural components of wood. Of the two biomacromolecules, lignin is considered a more promising aromatic source because it is the most abundant biopolymer present in nature. Due to its abundance and various extraction techniques, the commercial availability of lignin (1.1 million tons/year)[23] is significantly higher than that of tannins (0.2 million tons/year).[24] However, since lignin is highly branched and complex, significant challenges exist in characterizing and analyzing composite materials. To overcome these challenges, lignin depolymerization has been performed to break down lignin into monomeric aromatic compounds,[25−27] which can then be polymerized to create functional polymers with well-defined chemical structures and facile characterization.

Among the products obtained through lignin depolymerization, the product accounting for the largest volume is vanillin. Vanillin is well known as a flavoring agent in vanilla and is the only renewable aromatic compound produced on an industrial scale,[28] with an annual production of 3000 tons solely from lignin, and the total scale of vanillin production reaches 20,000 tons per year.[28] The chemical structure of vanillin consists of *o*-methoxyphenol, or guaiacol, with an attached aldehyde (Figure 1). The hydroxyl functional group in vanillin often serves as a starting point for chemical transformation, enabling the synthesis of biobased polymers. For example, vanillin can be

Received: October 10, 2023
Revised: January 7, 2024
Accepted: January 8, 2024
Published: January 19, 2024

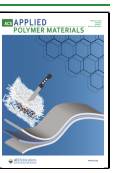

https://doi.org/10.1021/acsapm.3c02435
ACS Appl. Polym. Mater. 2024, 6, 1653−1661

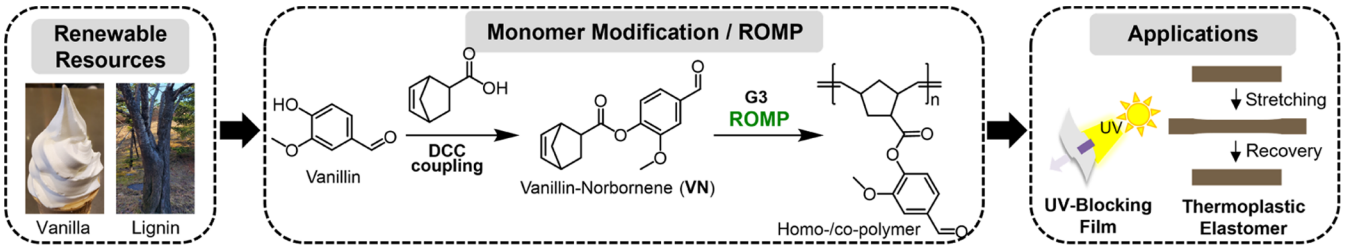

Figure 1. Overview of this work. Vanillin is a flavoring agent in vanilla and can be produced from lignin biomass. Chemically, vanillin contains a phenolic moiety, making it suitable for an *N*,*N*′-dicyclohexylcarbodiimide (DCC) coupling reaction to attach a norbornene moiety. This resulted in the formation of **VN**, which served as a ROMP monomer. Using **G3**, we can synthesize **pVN** and its copolymers, and their applications in UV-blocking films and thermoplastic elastomers (TPEs) will be discussed.

acrylated to form polymerizable vinyl monomers, which can then be polymerized using controlled radical polymerization techniques such as reversible addition−fragmentation chain transfer (RAFT) or atom transfer radical polymerization (ATRP) to produce functional polymers.[29−33] Additionally, by further cross-linking through the combination of aldehyde pendent groups of vanillin, biobased resins can be created.[34−37] While controlled radical polymerization offers many advantages, it also has inherent drawbacks, such as prolonged reaction times, high reaction temperatures, and chain transfer side reactions. In this context, ring-opening metathesis polymerization (ROMP)[38] can serve as an excellent alternative to radical polymerization. However, there has been limited research on the application of ROMP to vanillin derivatives. To the best of our knowledge, only one report discusses ROMP of vanillin derivatives, but this work involves multiple synthetic steps for ROMP and does not investigate the possibility of copolymerization.[39] This limitation has prompted us to explore the potential of ROMP by synthesizing a scalable ROMP monomer from vanillin and applying copolymerization.

We herein report the efficient transformation of biobased vanillin into homopolymers and triblock copolymers through ROMP for applications in UV-blocking films and high-performance TPEs (Figure 1). To achieve this, we first converted vanillin into vanillin 5-norbornene-2-carboxylate (**VN**), a ROMP-capable monomer, through Steglich esterification. **VN** was then polymerized using **G3** via ROMP, resulting in a glassy polynorbornene with a T_g of 95 °C, which could serve as a compelling alternative to petroleum-based polystyrene. Having confirmed the potential of ROMP, we utilized **VN** as a monomer for the hard block in triblock copolymer-based TPEs. In the TPE design, the monomers for the middle soft block contained *n*-butyl, *n*-octyl, or *n*-octyl having two methyl groups. The purpose of this study was to investigate the effect of alkyl chains on the TPE properties. Based on this design and by varying the weight percentages of the hard block, we successfully synthesized six vanillin-containing triblock copolymers. Phase separation was confirmed by atomic force microscopy (AFM), and their mechanical properties were investigated and compared to those of commercial TPE. These results highlight the great promise of vanillin-based TPEs as potential substitutes for conventional petrochemical-based TPEs.

2. MATERIALS AND METHODS

2.1. General. Chemicals were purchased from Sigma-Aldrich, TCI, Daejung Chemicals, Samchun Chemicals, and Duksan Chemicals without further purification, unless noted otherwise. All reactions were carried out under argon with standard Schlenk techniques. Reaction flasks were flame-dried. Dry solvents were prepared with activated 4 Å molecular sieves. Solvents for ROMP were degassed with Ar purging for 20 min. All ^{1}H NMR and ^{13}C NMR data are reported in ppm on a JEOL ECS 400 MHz NMR spectrometer. ^{1}H NMR is referenced to a chloroform peak (δ = 7.26 ppm). The multiplicity is reported as follows: s = singlet, d = doublet, dd = doublet of doublets, t = triplet, m = multiplet or unresolved, and br = broad. Coupling constants J are reported in hertz. ^{13}C NMR is referenced to a chloroform signal (δ = 77.16 ppm). High-resolution mass spectrometry (HRMS) using electrospray ionization (ESI) in positive mode was performed with an AB SCIEX Q-TOF 5600. A direct injection was performed, and the MS scan range was 100−2000 m/z. Gel permeation chromatography (GPC) was performed in tetrahydrofuran with a concentration of 2−3 mg/mL on a TOSOH HLC-8320 GPC. The GPC was calibrated with monodisperse polystyrene standards, and the data were analyzed using a refractive index detector. Dynamic light scattering (DLS) was performed in toluene by using an Otsuka ELSZ-2000ZS.

2.2. Thermal Analysis. Thermogravimetric analysis (TGA) was conducted using a TA Q50 instrument. The samples (6−9 mg) were heated at a rate of 20 °C/min from 30 to 600 °C under a nitrogen atmosphere. Differential scanning calorimetry (DSC) measurement was performed on a TA Instruments Q20. The samples (6−9 mg) were uniformly heated from −75 to 150 °C at a rate of 20 °C/min under a nitrogen atmosphere using Tzero hermetic pans.

2.3. Photophysical Analysis. UV−vis spectra were recorded on a Scinco Mega U600 UV−vis spectrophotometer at room temperature. To prepare the film, the polymer was first dissolved in dichloromethane (DCM). The resulting solution was transferred to a glass Petri dish and dried at room temperature for 2−3 days. The film was further dried in vacuo at 40 °C for 1 day.

2.4. Mechanical Analysis. Mechanical properties were analyzed by using a Universal Testing Machine (UTM, Lloyd LR30K Plus). The measurements were conducted with a 1 kN load cell and crosshead speeds of 5−15 mm/min. The sample size was 1 × 5 × 0.01 cm. The sample was prepared by using a solvent casting method. The polymer was dissolved in DCM at a concentration of 500 mg/3 mL. The solution was then poured into a Teflon mold and dried at room temperature for 1 day and further under vacuum for 3 h. For cyclic testing, 5 cycles of loading−unloading ranging from 0 to 50% strain were conducted using a 1 kN load cell with a crosshead speed of 10 mm/min.

2.5. Atomic Force Microscopy (AFM). AFM (Park system, Korea, NX10) with a noncontact or tapping mode was used to visualize the phase separation on a silicon wafer. To prepare for the sample, a 1 × 1 cm silicon wafer (p-type, LG Siltron, Korea) was washed with acetone and 2-propanol, after which the remaining solvent was removed by blowing with nitrogen gas. The cleaned wafer was then exposed to a UV ozone cleaner for 15 min. Subsequently, a polymer solution (1 wt % in toluene) was deposited onto the wafer, and spin-coating was performed at 2500 rpm for 60 s. The size of hard blocks within the sample was measured using the image processing software, ImageJ. Approximately 274 domains in **P6** were selected, and their sizes were averaged.

2.6. Synthesis of VN. In a Schlenk flask, 5-norbornene-2-carboxylic acid (21.72 mmol, 1.00 equiv, 3.00 g), vanillin (26.04 mmol, 1.2 equiv, 3.96 g), *N*,*N*′-dicyclohexylcarbodiimide (23.88 mmol, 1.1 equiv, 4.93 g), and 4-dimethylaminopyridine (2.16 mmol, 0.10 equiv, 256.26 mg) were dissolved in 48 mL of DCM. The reaction mixture was stirred at room temperature for 24 h. The reaction mixture was filtered using a

https://doi.org/10.1021/acsapm.3c02435
ACS Appl. Polym. Mater. 2024, 6, 1653−1661

Büchner funnel. The organic layer was washed with saturated sodium bicarbonate (30 mL × 2), dried with anhydrous $MgSO_4$, and evaporated in vacuo. The mixture was purified with column chromatography (hexane:ethyl acetate = 6:4), producing a white solid (5.37 g, 90% yield). Melting point: 83 °C. ^{1}H NMR (400 MHz, $CDCl_3$) δ 9.94 (s, 1H, two singlets from endo:exo (0.75:0.25) mixture), 7.51−7.44 (m, 2H), 7.22 (d, J = 7.8 Hz, 0.25H), 7.16 (d, J = 7.9 Hz, 0.75H), 6.27 (dd, J = 5.7, 3.0 Hz, 0.75H), 6.21 (dd, J = 5.6, 2.9 Hz, 0.25H), 6.18 (dd, J = 5.5, 3.0 Hz, 0.25H), 6.10 (dd, J = 5.6, 2.8 Hz, 0.75H), 3.89 (s, 3H, two singlets), 3.41 (s, 0.75H), 3.29−3.24 (m, 1H), 2.99 (s, 1H), 2.57−2.51 (m, 0.25H), 2.15−2.07 (m, 0.25H), 2.06−1.98 (m, 0.75H), 1.61 (d, J = 8.7 Hz, 0.25H), 1.58−1.49 (m, 2H), 1.37 (d, J = 8.1 Hz, 0.75H); ^{13}C NMR (101 MHz, $CDCl_3$) δ 191.2, 172.4, 152.2, 145.4, 138.1, 135.2, 132.4, 124.9, 123.6, 110.9, 56.1, 49.9, 46.2, 43.4, 42.8, 29.5; HRMS (ESI) calculated for $C_{16}H_{17}O_4$ ($[M + H]^+$) 273.1121; found, 273.1123.

2.7. Synthesis of Bu.[40] In a Schlenk flask, 5-norbornene-2-carboxylic acid (14.48 mmol, 1.00 equiv, 2.00 g), 1-butanol (17.37 mmol, 1.2 equiv, 1.29 g), *N*,*N*′-dicyclohexylcarbodiimide (15.92 mmol, 1.1 equiv, 3.29 g), and 4-dimethylaminopyridine (1.45 mmol, 0.10 equiv, 176.85 mg) were dissolved in 40 mL of DCM. The reaction mixture was stirred at room temperature for 20 h. The mixture was then filtered using a Büchner funnel. The organic layer was washed with saturated sodium bicarbonate (20 mL × 2), dried with anhydrous $MgSO_4$, and evaporated in vacuo. The mixture was purified with column chromatography (hexane:ethyl acetate = 12:1), producing a colorless liquid (2.34 g, 83% yield). ^{1}H NMR (400 MHz, $CDCl_3$) δ 6.18 (dd, J = 5.7, 3.0 Hz, 0.75H), 6.13 (dd, J = 5.6, 2.8 Hz, 0.25H), 6.10 (dd, J = 5.5, 3.0 Hz, 0.25H), 5.91 (dd, J = 5.6, 2.8 Hz, 0.75H), 4.12−3.96 (m, 2H), 3.20 (s, 0.75H), 3.03 (s, 0.25H), 2.97−2.86 (m, 1.75H), 2.23−2.17 (m, 0.25H), 1.97−1.84 (m, 1H), 1.65−1.50 (m, 2H), 1.45−1.32 (m, 4H), 1.31−1.22 (m, 1H), 0.98−0.88 (m, 3H).

2.8. Synthesis of Oct.[41] In a Schlenk flask, 5-norbornene-2-carboxylic acid (21.71 mmol, 1.00 equiv, 3.00 g), 1-octanol (26.06 mmol, 1.2 equiv, 3.39 g), *N*,*N*′-dicyclohexylcarbodiimide (23.88 mmol, 1.1 equiv, 4.93 g), and 4-dimethylaminopyridine (2.17 mmol, 0.10 equiv, 265.27 mg) were dissolved in 40 mL of DCM. The reaction mixture was stirred at room temperature for 20 h. The reaction mixture was then filtered using a Büchner funnel. The organic layer was washed with saturated sodium bicarbonate (40 mL × 2), dried with anhydrous $MgSO_4$, and evaporated in vacuo. The mixture was purified with column chromatography (hexane:ethyl acetate = 12:1), producing a colorless liquid (3.07 g, 56% yield). ^{1}H NMR (400 MHz, $CDCl_3$) δ 6.17 (dd, J = 5.7, 3.0 Hz, 0.75H), 6.12 (dd, J = 5.6, 2.8 Hz, 0.25H), 6.09 (dd, J = 5.5, 3.0 Hz, 0.25H), 5.90 (dd, J = 5.7, 2.8 Hz, 0.75H), 4.09−3.92 (m, 2H), 3.19 (s, 0.75H), 3.02 (s, 0.25H), 2.96−2.87 (m, 1.75H), 2.22−2.16 (m, 0.25H), 1.93−1.85 (m, 1H), 1.65−1.49 (m, 2H), 1.43−1.36 (m, 1H), 1.36−1.17 (m, 12H), 0.86 (t, J = 6.8 Hz, 3H).

2.9. Synthesis of BCOct.[42] In a Schlenk flask, 5-norbornene-2-carboxylic acid (21.71 mmol, 1.00 equiv, 3.00 g), 3,7-dimethyl-1-octanol (26.06 mmol, 1.2 equiv, 4.12 g), *N*,*N*′-dicyclohexylcarbodiimide (23.88 mmol, 1.1 equiv, 4.93 g), and 4-dimethylaminopyridine (2.17 mmol, 0.10 equiv, 265.27 mg) were dissolved in 40 mL of DCM. The reaction mixture was stirred at room temperature for 20 h. The reaction mixture was then filtered by using a Büchner funnel. The organic layer was washed with saturated sodium bicarbonate (40 mL × 2), dried with anhydrous $MgSO_4$, and evaporated in vacuo. The mixture was purified with column chromatography (hexane:ethyl acetate = 12:1), producing a colorless liquid (4.07 g, 67% yield). ^{1}H NMR (400 MHz, $CDCl_3$) δ 6.19 (dd, J = 5.6, 3.0 Hz, 0.75H), 6.14 (dd, J = 5.6, 2.9 Hz, 0.25H), 6.12−6.09 (m, 0.25H), 5.92 (dd, J = 5.6, 2.8 Hz, 0.75H), 4.13−4.00 (m, 2H), 3.20 (s, 0.75H), 3.03 (s, 0.25H), 2.96−2.92 (m, 1.75H), 2.21−2.15 (m, 0.25H), 1.95−1.86 (m, 1H), 1.67−1.58 (m, 1H), 1.55−1.48 (m, 2H), 1.44−1.19 (m, 7H), 1.17−1.10 (m, 3H), 0.91−0.85 (m, 9H).

2.10. Synthesis of G3. Grubbs' second-generation catalyst (589 μmol, 1.00 equiv, 500 mg) and pyridine (5.89 mmol, 10 equiv, 0.47 mL) were dissolved in 5 mL of toluene. The reaction mixture was stirred at room temperature for 1 h. The reaction mixture was precipitated by using 30 mL of hexane. The precipitates were filtered, thoroughly washed with hexane, and dried in vacuo at 35 °C. **G3** was obtained as a light green solid (354 mg, 83% yield).

2.11. Homopolymerization Procedure for pVN. To the Schlenk flask, **G3** (44.07 μmol, 1 equiv, 32.03 mg) was dissolved in 4.8 mL of DCM. Subsequently, the **VN** monomer (8.81 mmol, 200 equiv, 2.4 g) was added. The reaction was carried out at room temperature for 30 min, followed by quenching with EVE. The solution was precipitated twice using methanol. The precipitates were filtered, thoroughly washed with methanol, and dried in vacuo at 35 °C, producing a grayish-green solid (2.2 g, 92% conversion). ^{1}H NMR (400 MHz, $CDCl_3$) δ 10.01−9.73 (br, 1H), 7.55−7.27 (br, 2H), 7.21−6.97 (br, 1H), 5.76−5.26 (br, 2H), 3.93−3.62 (br, 3H), 3.29−3.18 (br, 0.75H), 3.07−2.85 (br, 1H), 2.66−2.55 (br, 0.25H), 2.33−2.11 (br, 1H), 1.97−1.89 (br, 1H), 1.70−1.41 (br, 3H); GPC (THF): M_n 49,000 g/mol, $Đ$ = 1.23.

2.12. Homopolymerization Procedures for pBu, pOct, and pBCOct. In a Schlenk flask, **G3** (**pBu**: 7.72 μmol, 1 equiv, 5.61 mg, **pOct**: 2.00 μmol, 1 equiv, 1.45 mg, **pBCOct**: 5.39 μmol, 1 equiv, 3.92 mg) was dissolved in 0.5 mL of DCM. The monomer (**pBu**: 1.54 mmol, 200 equiv, 300 mg, **pOct**: 0.40 mmol, 200 equiv, 100 mg, **pBCOct**: 1.08 mmol, 200 equiv, 300 mg) was dissolved in another 0.5 mL of DCM and was added to the **G3** solution. The mixture was stirred at room temperature for 30 min, followed by quenching with EVE. The polymer solution was precipitated twice in methanol. The precipitates were filtered, thoroughly washed with methanol, and dried in vacuo at 35 °C, affording a soft solid. **pBu**: ^{1}H NMR (400 MHz, $CDCl_3$) δ 5.54−5.10 (br, 2H), 4.16−3.90 (br, 2H), 3.27−3.00 (br, 0.75H), 2.97−2.73 (br, 1.5H), 2.70−2.33 (br, 0.75H), 2.16−1.82 (br, 2H), 1.81−1.66 (br, 1H), 1.63−1.54 (br, 2H), 1.45−1.10 (br, 3H), 0.99−0.85 (br, 3H); GPC (THF): M_n 40,000 g/mol, $Đ$ = 1.38. **pOct**: ^{1}H NMR (400 MHz, $CDCl_3$) δ 5.57−5.04 (br, 2H), 4.15−3.89 (br, 2H), 3.26−3.04 (br, 0.75H), 2.99−2.74 (br, 1.5H), 2.63−2.39 (br, 0.75H), 2.12−1.82 (br, 2H), 1.80−1.67 (br, 1H), 1.61−1.53 (br, 2H), 1.37−1.19 (br, 11H), 0.93−0.83 (br, 3H); GPC (THF): M_n 42,400 g/mol, $Đ$ = 1.13. **pBCOct**: ^{1}H NMR (400 MHz, $CDCl_3$) δ 5.55−5.06 (br, 2H), 4.23−3.89 (br, 2H), 3.25−2.98 (br, 0.75H), 2.95−2.69 (br, 1.5H), 2.67−2.35 (br, 0.75H), 2.15−1.83 (br, 2H), 1.82−1.67 (br, 1H), 1.64−1.45 (br, 4H), 1.42−1.36 (br, 1H), 1.32−1.20 (br, 3H), 1.16−1.08 (br, 3H), 0.92−0.83 (br, 9H); GPC (THF): M_n 49,600 g/mol, $Đ$ = 1.13.

2.13. Triblock Copolymerization Procedures for P1 and P4. In a Schlenk flask, **G3** (25.74 μmol, 1 equiv, 18.70 mg) was dissolved in 1.5 mL of DCM. **VN** (**P1**: 0.44 mmol, 17 equiv, 119.14 mg, **P4**: 0.77 mmol, 30 equiv, 210.24 mg) was dissolved in 3.5 mL of DCM and injected into the **G3** solution. The reaction mixture was stirred at room temperature for 1 h, followed by the addition of **Bu** (3.86 mmol, 150 equiv, 750 mg) dissolved in 5−6 mL of DCM for the second block. The mixture was then stirred for 4.5 h. The third block was formed by injecting **VN** (**P1**: 0.44 mmol, 17 equiv, 119.14 mg, **P4**: 0.77 mmol, 30 equiv, 210.24 mg), and the mixture was stirred for 14 h. The reaction was quenched using EVE. The polymer solution was precipitated twice in methanol. The precipitates were filtered, thoroughly washed with methanol, and dried in vacuo at 35 °C, affording a solid. **P1**: ^{1}H NMR (400 MHz, $CDCl_3$) δ 9.96−9.80 (br, 2H), 7.52−7.30 (br, 4H), 7.20−7.04 (br, 2H), 5.78−5.11 (br, 20H), 4.17−3.92 (br, 17H), 3.91−3.73 (br, 7H), 3.28−3.06 (br, 7H), 3.03−2.70 (br, 16H), 2.58−2.40 (br, 5H), 2.11−1.84 (br, 19H), 1.80−1.69 (br, 7H), 1.65−1.51 (br, 28H), 1.46−1.31 (br, 22H), 1.01−0.83 (br, 24H); GPC (THF): M_n 32,000 g/mol, $Đ$ = 1.35; conversion = 55.7%. **P4**: ^{1}H NMR (400 MHz, $CDCl_3$) δ 9.97−9.78 (br, 2H), 7.54−7.28 (br, 4H), 7.21−7.03 (br, 2H), 5.79−5.12 (br, 10H), 4.42−3.92 (br, 8H), 3.91−3.74 (br, 6H), 3.39−3.09 (br, 5H), 3.04−2.73 (br, 7H), 2.67−2.40 (br, 3H), 2.30−2.14 (br, 3H), 2.13−1.69 (br, 15H), 1.69−1.48 (br, 12H), 1.46−1.28 (br, 9H), 1.01−0.84 (br, 10H); GPC (THF): M_n 33,100 g/mol, $Đ$ = 1.40; conversion = 83.7%.

2.14. Triblock Copolymerization Procedures for P2 and P5. In a Schlenk flask, **G3** (19.97 μmol, 1 equiv, 14.51 mg) was dissolved in 1.5 mL of DCM. **VN** (**P2**: 0.60 mmol, 30 equiv, 163.13 mg, **P5**: 0.96 mmol, 48 equiv., 261.01 mg) was dissolved in another 3.5 mL of DCM, which was added to the **G3** solution. The reaction mixture was stirred at room temperature for 1 h. Then, **Oct** (3 mmol, 150 equiv, 750 mg),

https://doi.org/10.1021/acsapm.3c02435
ACS Appl. Polym. Mater. 2024, 6, 1653−1661

which was dissolved in 5−6 mL of DCM, was injected into the mixture to form the second block. After being stirred for 4.5 h, **VN** (**P2**: 0.60 mmol, 30 equiv, 163.13 mg, **P5**: 0.96 mmol, 48 equiv, 261.01 mg) was added to the mixture to form the third block and was stirred for 14 h. The reaction was quenched using EVE. The polymer solution was precipitated twice in methanol. The precipitates were filtered, thoroughly washed with methanol, and dried in vacuo at 35 °C, affording a solid. **P2**: ^{1}H NMR (400 MHz, $CDCl_3$) δ 9.96−9.81 (br, 2H), 7.59−7.28 (br, 4H), 7.20−7.01 (br, 2H), 5.82−5.13 (br, 15H), 4.27−3.90 (br, 11H), 3.88−3.76 (br, 6H), 3.32−3.04 (br, 6H), 3.01−2.69 (br, 11H), 2.58−2.39 (br, 3H), 2.33−2.15 (br, 3H), 2.12−1.81 (br, 15H), 1.80−1.70 (br, 5H), 1.69−1.49 (br, 20H), 1.46−1.19 (br, 59H), 0.96−0.80 (br, 15H); GPC (THF): M_n 40,200 g/mol, $Đ$ = 1.34; conversion = 71.7%. **P5**: ^{1}H NMR (400 MHz, $CDCl_3$) δ 10.03−9.72 (br, 2H), 7.51−7.29 (br, 4H), 7.20−7.03 (br, 2H), 5.83−5.10 (br, 11H), 4.24−3.91 (br, 6H), 3.90−3.74 (br, 6H), 3.39−3.08 (br, 5H), 3.04−2.71 (br, 8H), 2.67−2.40 (br, 3H), 2.35−2.11 (br, 3H), 2.10−1.83 (br, 10H), 1.81−1.69 (br, 4H), 1.69−1.49 (br, 17H), 1.43−1.18 (br, 36H), 0.98−0.76 (br, 9H); GPC (THF): M_n 50,700 g/mol, $Đ$ = 1.33; conversion = 81.4%.

2.15. Triblock Copolymerization Procedures for P3 and P6. In a Schlenk flask, **G3** (17.96 μmol, 1 equiv, 13.05 mg) was dissolved in 1.5 mL of DCM. **VN** (**P3**: 0.54 mmol, 30 equiv, 146.69 mg, **P6**: 0.93 mmol, 52 equiv, 254.27 mg) was dissolved in another 3.5 mL of DCM, which was added to the **G3** solution. The reaction mixture was stirred at room temperature for 1 h. Then, **BCOct** (2.69 mmol, 150 equiv, 750 mg), which was dissolved in 5−6 mL of DCM, was added to the mixture to form the second block. After the mixture was stirred for 4.5 h, **VN** (**P3**: 0.54 mmol, 30 equiv, 146.69 mg, **P6**: 0.93 mmol, 52 equiv, 254.27 mg) was added to the mixture to form the third block. The reaction was quenched using EVE. The polymer solution was precipitated twice in methanol. The precipitates were filtered, thoroughly washed with methanol, and dried in vacuo at 35 °C, affording a solid. **P3**: ^{1}H NMR (400 MHz, $CDCl_3$) δ 9.98−9.81 (br, 2H), 7.52−7.32 (br, 4H), 7.21−7.06 (br, 2H), 5.80−5.10 (br, 16H), 4.27−3.92 (br, 12H), 3.91−3.74 (br, 7H), 3.32−3.04 (br, 7H), 3.00−2.72 (br, 11H), 2.60−2.43 (br, 3H), 2.31−2.13 (br, 2H), 2.11−1.85 (br, 14H), 1.82−1.68 (br, 7H), 1.66−1.46 (br, 23H), 1.43−1.35 (br, 8H), 1.33−1.21 (br, 18H), 1.20−1.07 (br, 19H), 0.98−0.79 (br, 53H); GPC (THF): M_n 46,700 g/mol, $Đ$ = 1.27; conversion = 70.2%. **P6**: ^{1}H NMR (400 MHz, $CDCl_3$) δ 9.98−9.81 (br, 2H), 7.51−7.30 (br, 4H), 7.21−7.05 (br, 2H), 5.78−5.12 (br, 9H), 4.31−3.93 (br, 5H), 3.90−3.73 (br, 6H), 3.38−3.06 (br, 5H), 3.02−2.72 (br, 7H), 2.67−2.39 (br, 3H), 2.34−2.15 (br, 3H), 2.11−1.82 (br, 9H), 1.81−1.70 (br, 2H), 1.68−1.46 (br, 12H), 1.44−1.35 (br, 4H), 1.33−1.19 (br, 9H), 1.18−1.05 (br, 8H), 1.00−0.80 (br, 22H); GPC (THF): M_n 61,200 g/mol, $Đ$ = 1.24; conversion = 72.5%.

3. RESULTS AND DISCUSSION

We initiated this work by synthesizing a potential ROMP monomer using vanillin (Figure 2a). Due to the presence of a hydroxyl group in vanillin and the commercial availability of 5-norbornene-2-carboxylic acid (endo/exo mixture with an approximate ratio of 0.75:0.25), we employed a Steglich esterification reaction to form vanillin 5-norbornene-2-carboxylate (**VN**). The synthesis began by mixing 5-norbornene-2-carboxylic acid (1.0 equiv) and vanillin (1.2 equiv) in the presence of *N*,*N*′-dicyclohexylcarbodiimide (DCC, 1.1 equiv) and 4-dimethylaminopyridine (DMAP, 0.10 equiv) in dichloromethane (DCM) (Figure 2a). The isolated yield was 90%. **VN** was thoroughly characterized using ^{1}H NMR (Figure 2b), ^{13}C NMR, and high-resolution mass spectrometry (HRMS), all of which confirmed the chemical structure of **VN**. Next, we attempted the homopolymerization of **VN** using a Grubbs' third-generation catalyst (**G3**) (Figure 2a), resulting in the formation of poly(vanillin 5-norbornene-2-carboxylate) (**pVN**) with a molecular weight of 49,000 g/mol with a $Đ$ of 1.23 (the GPC trace is included in the Supporting Information). The

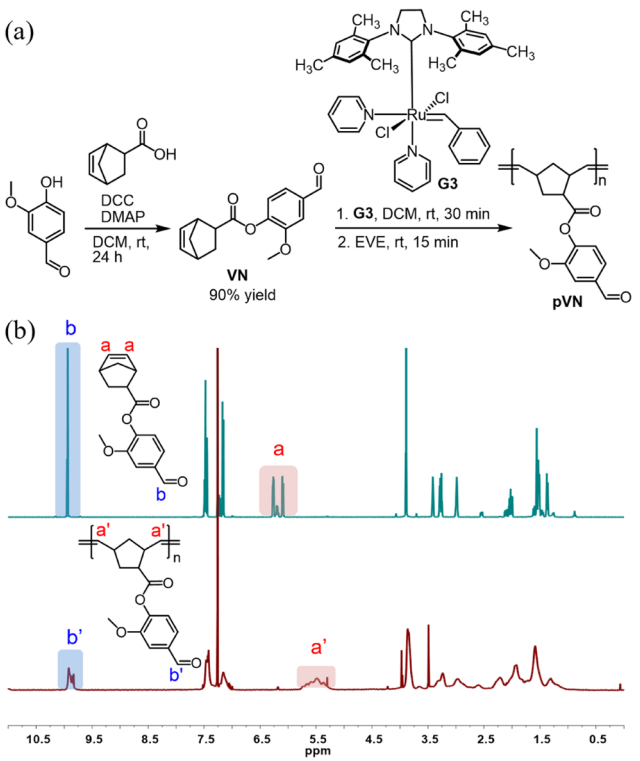

(c)

Sample	[VN]:[G3]	M_n (g/mol)	$Đ$	Conversion (%)(1)	T_g (°C)(2)	T_d (°C)(3)
pVN	200 : 1	49,000	1.23	92	95	242

Figure 2. Synthesis and characterization of **VN** and its homopolymer, **pVN**. (a) Synthetic scheme. **VN** was synthesized using vanillin and 5-norbornene-2-carboxylic acid. Subsequently, ROMP using **VN** and **G3** was performed, resulting in the formation of **pVN**. (b) ^{1}H NMR spectra of **VN** and **pVN**. A peak labeled as a disappeared, while a new broad peak labeled as a′ appeared. Raw data are included in the Supporting Information. (c) Summary of the properties of **pVN**. (1) Calculated based on the weight of the obtained polymer. (2) Glass transition temperature measured by DSC. (3) Decomposition temperature with 5% mass loss determined by TGA.

conversion was 92%, which was determined by the obtained weight of polymer. Comparison of the ^{1}H NMR spectra of **VN** and **pVN** (Figure 2b) shows that olefin signals in the norbornene, labeled as a at around 6.2 ppm, disappeared, while broad olefin signals in the polymer backbone (polynorbornene), labeled as a′, appeared at around 5.5 ppm. In addition, an aldehyde peak at 9.9 ppm (labeled as b) significantly broadened after polymerization, which is a clear indication of polymer formation. Thermal properties of **pVN** were characterized by using differential scanning calorimetry (DSC) and thermogravimetric analysis (TGA). The glass transition temperature (T_g) was measured to be 95 °C (Supporting Information). This value was almost identical to the previously reported T_g of poly(vanillin acrylate) ($T_g \approx 95$ °C for a M_n of 10,500 g/mol and a $Đ$ of 2.68).[33] The decomposition temperature with 5% mass loss was measured at 242 °C (Supporting Information). The color of **pVN** appeared grayish-green, suggesting the possible presence of residual Grubbs catalyst even after the ROMP was terminated by ethyl vinyl ether. This is a well-known phenomenon reported previously.[43] Inductively coupled plasma

https://doi.org/10.1021/acsapm.3c02435
ACS Appl. Polym. Mater. 2024, 6, 1653−1661

mass spectrometry (ICP-MS) analysis indicated a Ru content of 1071 mg/kg, suggesting that only 46% of Ru (excluding ligands) was removed after EVE quenching.

The high T_g value of **pVN** encouraged us to investigate its mechanical properties, which were determined by using a universal testing machine (UTM). Samples with dimensions of 1 × 5 × 0.01 cm were prepared using a solvent casting method. The stress−strain curve is presented in Figure 3a, from which we

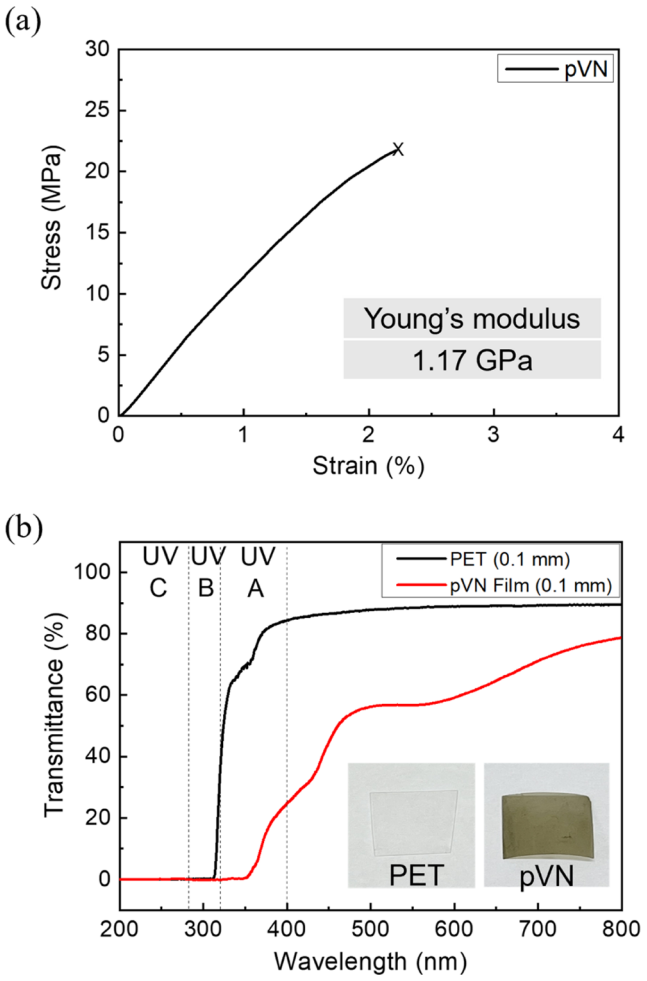

Figure 3. Application of **pVN**. (a) Uniaxial stress−strain curve for **pVN**. The Young's modulus was 1.17 GPa, indicating that this polymer was glassy at room temperature. (b) Transmittance of **pVN** film compared to PET film. The **pVN** film displayed superior performance in absorbing UV-A.

obtained a Young's modulus of 1.17 GPa and an elongation at break of 2.2%, confirming its stiff and rigid characteristics. Polystyrene and PET, commercial glassy polymers, are known to exhibit Young's moduli in the range of 2.4−3.2[44] and 2.5−2.8 GPa,[45] respectively, and thus, **pVN** could serve as a sustainable alternative to petroleum-based glassy polymers. Additionally, we examined the potential of **pVN** for use as UV-blocking films (Figure 3b). Lignin-based materials exhibited UV-blocking properties due to the presence of numerous aromatic rings,[21,46−48] and the same principle may also be applied to vanillin-based polymers. To assess these UV-blocking characteristics, we prepared **pVN** films through solvent casting with a thickness of approximately 0.1 mm. For comparison, we also used a commercially available PET film with a similar thickness. As shown in Figure 3b, a **pVN** film completely blocked UV-B (280−320 nm) and exhibited only an average transmittance of 9% within the UV-A range (320−400 nm). In contrast, a PET film showed partial transmission of UV-B and an average transmittance of 73% within UV-A. This result highlights the excellent UV-protective properties of **pVN** films, suggesting potential applications across various fields, such as sunscreens, food packaging, and windows. It is noted that the color of **pVN** films appeared grayish-green, as indicated by the absorption of visible light (Figure 3b). In contrast, the diluted solution of **VN** and **pVN** in chloroform showed no visible light absorption (Supporting Information) due to the absence of extended aromatics. Presumably, as mentioned above, a small amount of the residual Ru catalyst in green may exist due to incomplete ROMP termination, and the effect of the lightly colored catalyst becomes apparent in the solid state. Although some applications demand transparent colors for synthetic polymers, new chemistry aimed at near-complete ROMP termination could resolve this issue.[49]

Based on the glassy nature of **pVN**, we investigated the potential of ABA-type triblock copolymers containing **VN** monomers for applications in biobased TPEs. Several of our polymer design principles are as follows: (1) using **VN** as a hard end block and alkyl norbornene carboxylate as a soft middle block, (2) using three different alkyl norbornene carboxylates (*n*-butyl (**Bu**), *n*-octyl (**Oct**), or *n*-octyl having two methyl groups (**BCOct**, or branched octyl)) to examine the effect of alkyl chain length or branched alkyl chains on the mechanical properties, and (3) changing hard block weight percentages (one for ∼27 wt % and the other for ∼41 wt %) to investigate the effect of hard block contents on the mechanical properties. With these design principles in mind, we produced six vanillin-based TPEs (Figure 4). The six triblock copolymers, poly(**VN**-*b*-alkyl norbornene carboxylate-*b*-**VN**), were prepared through sequential addition of the corresponding norbornene monomers during ROMP (Figure 4a). In brief, **VN** was first polymerized in the presence of **G3** for 1 h, followed by the polymerization of the second block using alkyl norbornene carboxylate for 4.5 h, and last the third block using **VN** for 14 h. The reaction times for each block were determined by weighting complete conversions (preferred with longer reaction times) against preventing catalyst deactivation (preferred with shorter reaction times). Particularly, for the second block polymerization, a reaction of 1 h was insufficient (see the Supporting Information), prompting us to consider a longer reaction time.[50] Next, to confirm the formation of triblock copolymers, a small amount of the solution in a model polymer reaction was taken out before the injection of the next monomers, quenched by ethyl vinyl ether (EVE), precipitated, and subjected to GPC analysis. The increasing molecular weights of homo-, di-, and triblock copolymers implied successful chain extension (see the Supporting Information). Having confirmed the triblock copolymerization using ROMP, we prepared a total of six triblock copolymers, and the summary of these polymers is shown in Figure 4b (^{1}H NMR and GPC traces are shown in the Supporting Information). As a representative example, photos of **P1** in two different states (bulk and film) are shown (Figure 4c). The hard block weight percentages of the **P1**−**P3** series were determined to be 25−29 wt %, while those of the **P4**−**P6** series were 41−42 wt % (detailed calculations are outlined in the Supporting Information). These weight percentages were controlled by adding appropriate amounts of the soft block monomers in reference to **VN**. **P1**/**P4**, **P2**/**P5**, and **P3**/**P6** contain the soft blocks of **Bu**,

https://doi.org/10.1021/acsapm.3c02435
ACS Appl. Polym. Mater. 2024, 6, 1653−1661

(a)

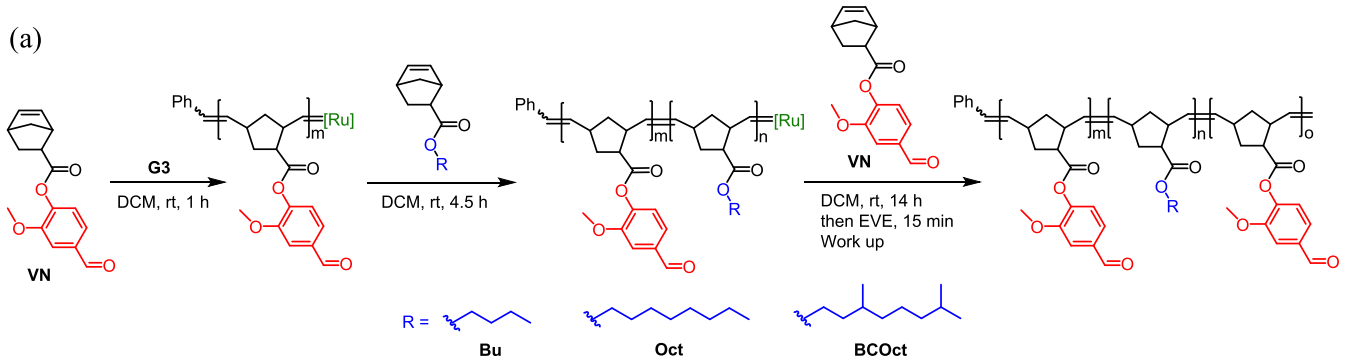

(b)

Name	ABA-Type Triblock Composition	Hard Block (wt %)	Vanillin (wt %)	M_n (g/mol)	$Đ$	Conversion (%)	$T_{g,1}$ / $T_{g,2}$ (°C)	T_d (°C)
P1	**VN**-*b*-**Bu**-*b*-**VN**	25.2	14.0	32,000	1.35	55.7	8 / 86	323
P2	**VN**-*b*-**Oct**-*b*-**VN**	29.3	16.3	40,200	1.34	71.7	-35 / 86	242
P3	**VN**-*b*-**BCOct**-*b*-**VN**	24.9	13.8	46,700	1.27	70.2	-31 / 96	273
P4	**VN**-*b*-**Bu**-*b*-**VN**	42.1	23.4	33,100	1.40	83.7	9 / 90	259
P5	**VN**-*b*-**Oct**-*b*-**VN**	40.8	22.7	50,700	1.33	81.4	-28 / 94	279
P6	**VN**-*b*-**BCOct**-*b*-**VN**	41.9	23.2	61,200	1.24	72.5	-27 / 94	264

(c)

Figure 4. Synthesis of poly(**VN**-*b*-alkyl norbornene carboxylate-*b*-**VN**) triblock copolymers. (a) Synthetic route. Triblock copolymers were synthesized through sequential monomer addition in ROMP. The values of m, n, and o are as follows (m/n/o): **P1** (15/123/15), **P2** (22/114/22), **P3** (21/126/21), **P4** (26/99/26), **P5** (38/120/38), and **P6** (48/127/48). It is assumed that the values of m and o are identical. (b) Summarized data for triblock copolymers. (c) Photographs of **P1** in the bulk (left) and the film state (right). Conversion, T_g, and T_d were obtained using the same methods as in Figure 2.

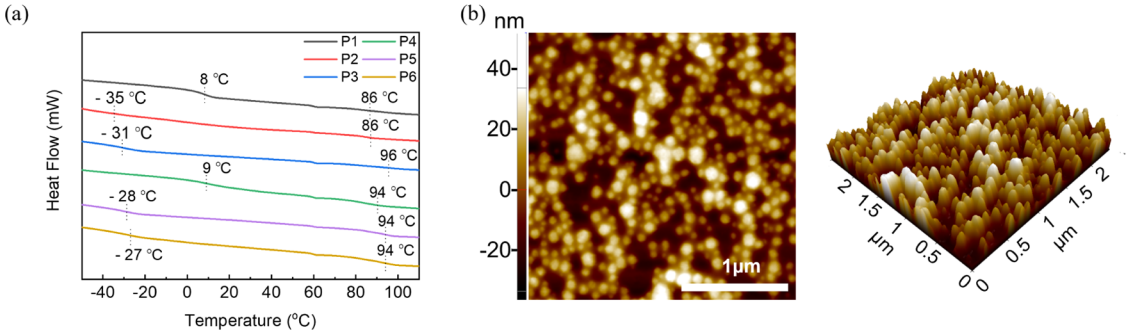

Figure 5. Characterization for microphase separation. (a) DSC thermograms of the triblock copolymers (**P1**−**P6**). We observed two glass transition temperatures that can be attributed to two distinct domains. (b) Representative AFM images (2.5 × 2.5 μm) of **P6** in two-dimensional (2D) (left) and three-dimensional (3D) (right). The average size of the hard block domains was calculated to be 84 nm.

Oct, and **BCOct**, respectively. The molecular weights of **P1**−**P6** ranged from 32,000 to 61,200 g/mol, and the $Đ$ values were generally low (≤1.4), indicating successful control of ROMP. An increasing trend in triblock copolymer molecular weights (**P1** → **P2** → **P3** or **P4** → **P5** → **P6**) was observed as the alkyl chain length increased. Vanillin contents ranged from 13.8 to 23.4 wt % (calculation is included in the Supporting Information). The aldehyde functional groups in vanillin were observed and were reactive toward primary amines, forming imine bonds (see the Supporting Information). DSC analysis of **P1**−**P6** indicated two distinct T_g values (*vide infra*).

TPEs are generally composed of phase-separated ABA-type triblock copolymers. Hard blocks provide physical cross-links, while soft blocks offer flexibility and elasticity.[51] The phase separation of the triblock copolymers was confirmed by using DSC and AFM (Figure 5). In the DSC thermograms, two distinct T_g values were observed in each polymer (Figure 5a). This double T_g generally occurs when there are two distinct polymer domains having different T_g values.[52,53] Specifically, we observed high T_g values ranging from 86 to 96 °C for **P1**−**P6**, which can be attributed to the **pVN** domains, given the T_g of the **pVN** homopolymer measured at 95 °C. It is also worth noting that for **P1**−**P3**, T_g was not distinctly observed, possibly due to the relatively low wt % of the **pVN** chains, as reported previously.[54] In contrast, for **P4**−**P6** with a high wt % of vanillin, T_g was clearly observed and was closer to the T_g of the **pVN** homopolymer. For the soft blocks, to accurately characterize the T_g, we separately synthesized homopolymers consisting of soft blocks: poly(*n*-butyl norbornene carboxylate) (**pBu**), poly(*n*-octyl norbornene carboxylate) (**pOct**), and poly(branched *n*-octyl norbornene carboxylate) (**pBCOct**). Their ^{1}H NMR spectra, GPC traces, and DSC thermograms are included in the

https://doi.org/10.1021/acsapm.3c02435
ACS Appl. Polym. Mater. 2024, 6, 1653−1661

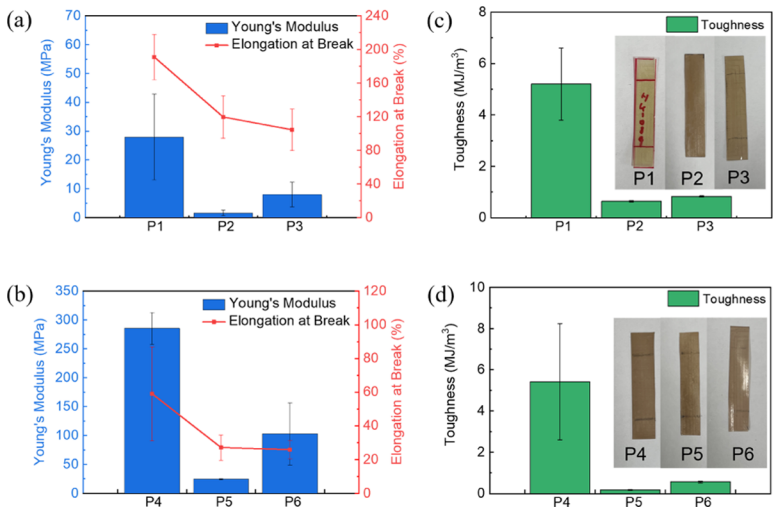

(e)

Entry	Young's modulus [MPa]	Elongation at break [%]	Toughness [MJ/m³]
P1	28.0 ± 14.9	191 ± 27	5.21 ± 1.4
P2	1.6 ± 1.0	120 ± 25	0.64 ± 0.03
P3	8.0 ± 4.3	104 ± 25	0.83 ± 0.02
P4	285 ± 27.4	59 ± 28	5.42 ± 2.82
P5	24.6 ± 1.0	27 ± 7	0.18 ± 0.02
P6	103 ± 53.6	26 ± 5	0.56 ± 0.05

Figure 6. (a, b) Young's moduli and elongation at break of **P1**−**P6**. (c, d) Toughness of **P1**−**P6**. The photos of each sample are included in the insets. (e) Summary of the mechanical properties. **P1** indicated excellent Young's modulus and elongation at break.

Supporting Information. The T_g values of the three homopolymers were obtained as follows: −3 (**pBu**), −34 (**pOct**), and −31 °C (**pBCOct**). These homopolymer T_g values were consistent with those of the corresponding triblock copolymers (**P1**/**P4** for **pBu**, **P2**/**P5** for **pOct**, and **P3**/**P6** for **pBCOct**), demonstrating the presence of the respective phase-separated soft blocks.

To further examine the phase separation, we employed AFM to visualize microphase separation (see Figure 5b for **P6** and the Supporting Information for **P1**−**P5**). For sample preparation, a 1 wt % of **P6** solution was spin-coated onto a silicon wafer, and AFM images were acquired using a noncontact or tapping mode. The brighter regions corresponded to the hard block domains composed of vanillin, while the darker regions represented the soft block composed of branched octyl chains. The average size of the hard domains in **P6** was calculated to be 84 nm, with the distribution ranging from 32 to 175 nm. Dynamic light scattering data for **P1**−**P6** in toluene also indicated the particle (potentially micelle) formation with the size ranging from 83 to 143 nm (Supporting Information). In the previous study, polynorbornene-based triblock copolymers with an M_n of 70,200 g/mol and a $Đ$ of 1.18 exhibited an average feature size of 106 nm, which is in good agreement with our AFM results.[55] These DSC, AFM, and DLS data clearly demonstrate microphase separation, indicating great potential for use as TPEs (*vide infra*).

Given the phase separation, we examined the mechanical properties of **P1**−**P6** (Figures 6 and S11). Polymer samples with dimensions of 1 × 5 cm were prepared using the solution casting method, and a UTM was used to measure the Young's modulus, elongation at break, and toughness of each sample. In both the **P1**−**P3** (≈27 wt % of hard block) and **P4**−**P6** (≈41 wt % of hard block) series, we observed that the soft blocks containing *n*-butyl exhibited superior Young's moduli (28 MPa for **P1** and 285 MPa for **P4**) compared to *n*-octyl (1.6 MPa for **P2** and 24.6 MPa for **P5**) and branched *n*-octyl (8.0 MPa for **P3** and 103 MPa for **P6**) (Figure 6a,b, blue). **P1** and **P4** containing *n*-butyl soft blocks also indicated high values of elongation at break (Figure 6a,b, red), which was unexpected because hard materials are generally brittle. This C4 chain may be short enough to maintain the mechanical strength and long enough to allow for elongation. This advantageous short−long balance may be disrupted when the carbon chain becomes longer. The high Young's moduli and elongation at break of **P1** and **P4** result in higher values of toughness (Figure 6c,d). Specifically, **P1** and **P4** showed toughness of more than 5 MJ/m^3, whereas **P2**, **P3**, **P5**, and **P6** had toughness of less than 1 MJ/m^3. The similar toughness of **P1** and **P4** strongly suggests that vanillin-based TPEs with varying Young's modulus and elongation can be prepared simply by changing the weight percentages of vanillin contents in triblock copolymers while maintaining the toughness of the materials.

Due to the excellent mechanical properties, we compared **P1** (25 wt % of hard block) with the commercial TPE, poly(styrene-*b*-isoprene-*b*-styrene) (SIS), in the literature. The SIS (22 wt % of hard block) indicated a Young's modulus of 3.6 MPa and elongation at break of about 700%, showing that **P1** exhibited about 7.8 times higher modulus with 3.7 times less elongation than those of SIS.[56] Although the elongation at break of **P1** is less than that of SIS, we believe that the tailored hard/soft ratio could improve the elongation by sacrificing the modulus, considering the higher modulus of **P1** compared to that of SIS.

We also tested the recovery of **P1** after elongation. We observed the complete recovery of **P1** after elongation at 50% strain for several hours. We then elongated **P1** until fracture and monitored its shrinking in a quantitative way (Figure S12). In this experiment, the strain of **P1** at fracture was 228% (3 → 9.85 cm), and **P1** instantly shrunk to almost half (63%, 4.9 cm) in 10 min. The material finally shrank back to 3.5 cm (originally 3 cm) in 22 h. This excellent power of recovery led us to investigate the cyclic loading−unloading test (Figure S13). In this cyclic test, **P1** was extended (at 50% strain) and shrunk, which was repeated five times, and the corresponding stress−strain curves were recorded. The material generally indicated reversible cycles after the first run. About 32% of residual deformation was observed after the fourth cycle due to the long relaxation time of **P1** at room temperature. Overall, the properties of **P1** were superior to the commercial petrochemical-based SIS in certain criteria, such as Young's modulus, suggesting great promise in the sustainable production of TPEs.

4. CONCLUSIONS

In this study, we report the efficient chemical conversion of biobased vanillin to vanillin 5-norbornene-2-carboxylate (**VN**),

https://doi.org/10.1021/acsapm.3c02435
ACS Appl. Polym. Mater. 2024, 6, 1653−1661

a ROMP-capable monomer. This **VN** was used in the synthesis of glassy **pVN** homopolymers and triblock copolymers employing soft comonomers for TPE applications. The glassy **pVN** exhibited a Young's modulus of 1.17 GPa, which could potentially substitute conventional perto-chemical polymers such as polystyrene and PET. The UV-blocking properties of **pVN** were also investigated. Following this homopolymer, we used **VN** in the triblock copolymers for TPE applications. Successful synthesis of triblock copolymers was achieved via the sequential addition of monomers in ROMP. We revealed that the soft comonomer containing *n*-butyl displayed the best performance as a TPE, surpassing commercial SIS in terms of Young's modulus. Although an extensive amount of biobased polymer research exists, to the best of our knowledge, **VN** was synthesized in this work for the first time, and its potential as a homopolymer and triblock copolymer was scrutinized. We are currently investigating other types of biobased feedstocks and their conversion to enable ROMP for various applications.

■ ASSOCIATED CONTENT

Supporting Information

The Supporting Information is available free of charge at https://pubs.acs.org/doi/10.1021/acsapm.3c02435.

GPC, TGA, DSC, photos of **pVN**, calculation of hard block and vanillin weight percentages, UTM, AFM, DLS, and NMR (PDF)

■ AUTHOR INFORMATION

Corresponding Author

Byungjin Koo − *Department of Polymer Science and Engineering, Dankook University, Yongin, Gyeonggi 16890, Republic of Korea;* orcid.org/0000-0003-0681-8084; Email: bkoo@dankook.ac.kr

Complete contact information is available at: https://pubs.acs.org/10.1021/acsapm.3c02435

Notes

The author declares no competing financial interest.

■ ACKNOWLEDGMENTS

The author thanks Haneul Kim and Sumin Lee for their experimental assistance. This work was supported by the National Research Foundation of Korea (NRF) grant funded by the Korean government (MSIT) (RS-2023-00210090).

■ REFERENCES

(1) Rosenboom, J.-G.; Langer, R.; Traverso, G. Bioplastics for a circular economy. *Nat. Rev. Mater.* **2022**, *7* (2), 117−137.

(2) Vennestrøm, P. N. R.; Osmundsen, C. M.; Christensen, C. H.; Taarning, E. Beyond Petrochemicals: The Renewable Chemicals Industry. *Angew. Chem., Int. Ed.* **2011**, *50* (45), 10502−10509.

(3) Hillmyer, M. A. The promise of plastics from plants. *Science* **2017**, *358* (6365), 868−870.

(4) Della Monica, F.; Kleij, A. W. From terpenes to sustainable and functional polymers. *Polym. Chem.* **2020**, *11* (32), 5109−5127.

(5) Miao, S.; Wang, P.; Su, Z.; Zhang, S. Vegetable-oil-based polymers as future polymeric biomaterials. *Acta Biomater.* **2014**, *10* (4), 1692−1704.

(6) Galbis, J. A.; García-Martín, M. d. G.; de Paz, M. V.; Galbis, E. Synthetic Polymers from Sugar-Based Monomers. *Chem. Rev.* **2016**, *116* (3), 1600−1636.

(7) Gandini, A.; Lacerda, T. M. From monomers to polymers from renewable resources: Recent advances. *Prog. Polym. Sci.* **2015**, *48*, 1−39.

(8) Gandini, A.; Lacerda, T. M.; Carvalho, A. J. F.; Trovatti, E. Progress of Polymers from Renewable Resources: Furans, Vegetable Oils, and Polysaccharides. *Chem. Rev.* **2016**, *116* (3), 1637−1669.

(9) Miller, S. A. Sustainable Polymers: Opportunities for the Next Decade. *ACS Macro Lett.* **2013**, *2* (6), 550−554.

(10) Zhu, Y.; Romain, C.; Williams, C. K. Sustainable polymers from renewable resources. *Nature* **2016**, *540* (7633), 354−362.

(11) Zhang, X.; Fevre, M.; Jones, G. O.; Waymouth, R. M. Catalysis as an Enabling Science for Sustainable Polymers. *Chem. Rev.* **2018**, *118* (2), 839−885.

(12) Cywar, R. M.; Rorrer, N. A.; Hoyt, C. B.; Beckham, G. T.; Chen, E. Y. X. Bio-based polymers with performance-advantaged properties. *Nat. Rev. Mater.* **2022**, *7* (2), 83−103.

(13) Mohanty, A. K.; Wu, F.; Mincheva, R.; Hakkarainen, M.; Raquez, J.-M.; Mielewski, D. F.; Narayan, R.; Netravali, A. N.; Misra, M. Sustainable polymers. *Nat. Rev. Methods Primers* **2022**, *2* (1), 46.

(14) Rasal, R. M.; Janorkar, A. V.; Hirt, D. E. Poly(lactic acid) modifications. *Prog. Polym. Sci.* **2010**, *35* (3), 338−356.

(15) Balla, E.; Daniilidis, V.; Karlioti, G.; Kalamas, T.; Stefanidou, M.; Bikiaris, N. D.; Vlachopoulos, A.; Koumentakou, I.; Bikiaris, D. N. Poly(lactic Acid): A Versatile Biobased Polymer for the Future with Multifunctional Properties—From Monomer Synthesis, Polymerization Techniques and Molecular Weight Increase to PLA Applications. *Polymers* **2021**, *13*, No. 1822.

(16) Nagarajan, D.; Nandini, A.; Dong, C.-D.; Lee, D.-J.; Chang, J.-S. Lactic Acid Production from Renewable Feedstocks Using Poly(vinyl alcohol)-Immobilized Lactobacillus plantarum 23. *Ind. Eng. Chem. Res.* **2020**, *59* (39), 17156−17164.

(17) Singhvi, M. S.; Zinjarde, S. S.; Gokhale, D. V. Polylactic acid: synthesis and biomedical applications. *J. Appl. Microbiol.* **2019**, *127* (6), 1612−1626.

(18) Li, G.; Zhao, M.; Xu, F.; Yang, B.; Li, X.; Meng, X.; Teng, L.; Sun, F.; Li, Y. Synthesis and Biological Application of Polylactic Acid. *Molecules* **2020**, *25* (21), 5023.

(19) Wang, J.; Liu, S.; Huang, J.; Qu, Z. A review on polyhydroxyalkanoate production from agricultural waste Biomass: Development, Advances, circular Approach, and challenges. *Bioresour. Technol.* **2021**, *342*, No. 126008.

(20) Iwata, T. Biodegradable and Bio-Based Polymers: Future Prospects of Eco-Friendly Plastics. *Angew. Chem., Int. Ed.* **2015**, *54* (11), 3210−3215.

(21) Zhang, Y.; Naebe, M. Lignin: A Review on Structure, Properties, and Applications as a Light-Colored UV Absorber. *ACS Sustainable Chem. Eng.* **2021**, *9* (4), 1427−1442.

(22) Arbenz, A.; Avérous, L. Chemical modification of tannins to elaborate aromatic biobased macromolecular architectures. *Green Chem.* **2015**, *17* (5), 2626−2646.

(23) Laurichesse, S.; Avérous, L. Chemical modification of lignins: Towards biobased polymers. *Prog. Polym. Sci.* **2014**, *39* (7), 1266−1290.

(24) Pizzi, A. Tannins: Major Sources, Properties and Applications. In *Monomers, Polymers and Composites from Renewable Resources*; Belgacem, M. N.; Gandini, A., Eds.; Elsevier: Amsterdam, 2008; Chapter 8, pp 179−199.

(25) Li, C.; Zhao, X.; Wang, A.; Huber, G. W.; Zhang, T. Catalytic Transformation of Lignin for the Production of Chemicals and Fuels. *Chem. Rev.* **2015**, *115* (21), 11559−11624.

(26) Sun, Z.; Fridrich, B.; de Santi, A.; Elangovan, S.; Barta, K. Bright Side of Lignin Depolymerization: Toward New Platform Chemicals. *Chem. Rev.* **2018**, *118* (2), 614−678.

(27) Schutyser, W.; Renders, T.; Van den Bosch, S.; Koelewijn, S. F.; Beckham, G. T.; Sels, B. F. Chemicals from lignin: an interplay of lignocellulose fractionation, depolymerisation, and upgrading. *Chem. Soc. Rev.* **2018**, *47* (3), 852−908.

(28) Fache, M.; Boutevin, B.; Caillol, S. Vanillin Production from Lignin and Its Use as a Renewable Chemical. *ACS Sustainable Chem. Eng.* **2016**, *4* (1), 35−46.

(29) Holmberg, A. L.; Stanzione, J. F., III; Wool, R. P.; Epps, T. H., III A Facile Method for Generating Designer Block Copolymers from

Functionalized Lignin Model Compounds. *ACS Sustainable Chem. Eng.* **2014**, *2* (4), 569−573.
(30) Fouilloux, H.; Qiang, W.; Robert, C.; Placet, V.; Thomas, C. M. Multicatalytic Transformation of (Meth)acrylic Acids: a One-Pot Approach to Biobased Poly(meth)acrylates. *Angew. Chem., Int. Ed.* **2021**, *60* (35), 19374−19382.
(31) Parkatzidis, K.; Boner, S.; Wang, H. S.; Anastasaki, A. Photoinduced Iron-Catalyzed ATRP of Renewable Monomers in Low-Toxicity Solvents: A Greener Approach. *ACS Macro Lett.* **2022**, *11* (7), 841−846.
(32) Tang, P.; Wang, Z.; Wen, C.; Yin, C.; Xing, Y.; Tai, H.; Jiang, F. Sustainable Multiblock Copolymer Elastomers Derived from Lignin with Tunable Performance toward Strong Adhesives and UV-Shielding Materials. *ACS Sustainable Chem. Eng.* **2023**, *11* (32), 11790−11798.
(33) Zhou, J.; Zhang, H.; Deng, J.; Wu, Y. High Glass-Transition Temperature Acrylate Polymers Derived from Biomasses, Syringaldehyde, and Vanillin. *Macromol. Chem. Phys.* **2016**, *217* (21), 2402−2408.
(34) Xu, Y.; Odelius, K.; Hakkarainen, M. Photocurable, Thermally Reprocessable, and Chemically Recyclable Vanillin-Based Imine Thermosets. *ACS Sustainable Chem. Eng.* **2020**, *8* (46), 17272−17279.
(35) Saito, K.; Eisenreich, F.; Türel, T.; Tomović, Ž. Closed-Loop Recycling of Poly(Imine-Carbonate) Derived from Plastic Waste and Bio-based Resources. *Angew. Chem., Int. Ed.* **2022**, *61* (43), No. e202211806.
(36) Wang, C.; Eisenreich, F.; Tomović, Ž. Closed-Loop Recyclable High-Performance Polyimine Aerogels Derived from Bio-Based Resources. *Adv. Mater.* **2023**, *35* (8), No. 2209003.
(37) Zhou, W.; Wang, W.; Shi, H.; Zeng, X.; Li, J.; Pang, Y.; Chang, Y.-C.; Sun, R.; Ren, L. Multiway Softness Polyurethane Elastomeric Composite with Enhanced Thermal Conductivity and Application as Thermal Interface Materials. *Adv. Mater. Technol.* **2023**, *8* (9), No. 2201701.
(38) Bielawski, C. W.; Grubbs, R. H. Living ring-opening metathesis polymerization. *Prog. Polym. Sci.* **2007**, *32* (1), 1−29.
(39) Naguib, M.; Yassin, M. A. Polymeric Antioxidant via ROMP of Bioderived Tricyclic Oxanorbornene Based on Vanillin and Furfurylamine. *ACS Appl. Polym. Mater.* **2022**, *4* (3), 2181−2188.
(40) Gumbley, P.; Hu, X.; Lawrence, J. A., III; Thomas Iii, S. W. Photoresponsive Gels Prepared by Ring-Opening Metathesis Polymerization. *Macromol. Rapid Commun.* **2013**, *34* (23−24), 1838−1843.
(41) Pollino, J. M.; Nair, K. P.; Stubbs, L. P.; Adams, J.; Weck, M. Cross-linked and functionalized 'universal polymer backbones' via simple, rapid, and orthogonal multi-site self-assembly. *Tetrahedron* **2004**, *60* (34), 7205−7215.
(42) Engelen, S.; Droesbeke, M.; Aksakal, R.; Du Prez, F. E. Ring-Opening Metathesis Polymerization for the Synthesis of Terpenoid-Based Pressure-Sensitive Adhesives. *ACS Macro Lett.* **2022**, *11* (12), 1378−1383.
(43) Vougioukalakis, G. C. Removing Ruthenium Residues from Olefin Metathesis Reaction Products. *Chem. - Eur. J.* **2012**, *18* (29), 8868−8880.
(44) Saito, M.; Ito, K.; Yokoyama, H. Mechanical Properties of Ultrathin Polystyrene-b-Polybutadiene-b-Polystyrene Block Copolymer Films: Film Thickness-Dependent Young's Modulus. *Macromolecules* **2021**, *54* (18), 8538−8547.
(45) Bin, Y.; Oishi, K.; Yoshida, K.; Matsuo, M. Mechanical Properties of Poly(ethylene terephthalate) Estimated in Terms of Orientation Distribution of Crystallites and Amorphous Chain Segments under Simultaneous Biaxially Stretching. *Polym. J.* **2004**, *36* (11), 888−898.
(46) Sadeghifar, H.; Venditti, R.; Jur, J.; Gorga, R. E.; Pawlak, J. J. Cellulose-Lignin Biodegradable and Flexible UV Protection Film. *ACS Sustainable Chem. Eng.* **2017**, *5* (1), 625−631.
(47) Sadeghifar, H.; Ragauskas, A. Lignin as a UV Light Blocker—A Review. *Polymers* **2020**, *12* (5), 1134.
(48) Tran, M. H.; Phan, D.-P.; Lee, E. Y. Review on lignin modifications toward natural UV protection ingredient for lignin-based sunscreens. *Green Chem.* **2021**, *23* (13), 4633−4646.
(49) Sui, X.; Wang, C.; Gutekunst, W. R. Sequestration of ruthenium residues via efficient fluorous-enyne termination. *Polym. Chem.* **2023**, *14* (27), 3160−3165.
(50) Belfield, K. D.; Zhang, L. Norbornene-Functionalized Diblock Copolymers via Ring-Opening Metathesis Polymerization for Magnetic Nanoparticle Stabilization. *Chem. Mater.* **2006**, *18* (25), 5929−5936.
(51) Voorhaar, L.; Diaz, M. M.; Leroux, F.; Rogers, S.; Abakumov, A. M.; Van Tendeloo, G.; Van Assche, G.; Van Mele, B.; Hoogenboom, R. Supramolecular thermoplastics and thermoplastic elastomer materials with self-healing ability based on oligomeric charged triblock copolymers. *NPG Asia Mater.* **2017**, *9* (5), e385.
(52) Kang, K.-S.; Phan, A.; Olikagu, C.; Lee, T.; Loy, D. A.; Kwon, M.; Paik, H.-j.; Hong, S. J.; Bang, J.; Parker Jr, W. O.; Sciarra, M.; de Angelis, A. R.; Pyun, J. Segmented Polyurethanes and Thermoplastic Elastomers from Elemental Sulfur with Enhanced Thermomechanical Properties and Flame Retardancy. *Angew. Chem., Int. Ed.* **2021**, *60* (42), 22900−22907.
(53) Luo, Y.; Wang, X.; Zhu, Y.; Li, B.-G.; Zhu, S. Polystyrene-block-poly(n-butyl acrylate)-block-polystyrene Triblock Copolymer Thermoplastic Elastomer Synthesized via RAFT Emulsion Polymerization. *Macromolecules* **2010**, *43* (18), 7472−7481.
(54) Gallagher, J. J.; Hillmyer, M. A.; Reineke, T. M. Acrylic Triblock Copolymers Incorporating Isosorbide for Pressure Sensitive Adhesives. *ACS Sustainable Chem. Eng.* **2016**, *4* (6), 3379−3387.
(55) Ganewatta, M. S.; Ding, W.; Rahman, M. A.; Yuan, L.; Wang, Z.; Hamidi, N.; Robertson, M. L.; Tang, C. Biobased Plastics and Elastomers from Renewable Rosin via "Living" Ring-Opening Metathesis Polymerization. *Macromolecules* **2016**, *49* (19), 7155−7164.
(56) Hosoya, R.; Ito, M.; Nakajima, K.; Morita, H. Coarse-Grained Molecular Dynamics Study of Styrene-block-isoprene-block-styrene Thermoplastic Elastomer Blends. *ACS Appl. Polym. Mater.* **2022**, *4* (4), 2401−2413.

https://doi.org/10.1021/acsapm.3c02435
ACS Appl. Polym. Mater. 2024, 6, 1653−1661